

**SCATTERING OF PULSED RADIATION FROM AN IMPERFECTLY-
CONDUCTING INFINITE PERIODIC SEA SURFACE**

J. Song, A. Norman, D. Nyquist, J. Ross, P. Ilavarasan,
M. Seneski, K. Chen and E. Rothwell
Department of Electrical Engineering
Michigan State University
East Lansing, Michigan 48824

The scattering of pulsed electromagnetic radiation from an imperfectly-conducting, infinite, periodic sea surface is studied. Such scattering influences the performance of impulse radars operating in a sea-surface environment. The time-domain transient response is synthesized from frequency-domain transfer functions for the induced surface and scattered fields. The two-medium scattering problem consists of space and sea-water regions separated by a periodic sea surface and illuminated by a plane wave incident from the space region. It is assumed that the space region (1) is located above sea-surface contour C , with permittivity $\epsilon_1 = \epsilon_0$. The sea-water region (2) is located below sea-surface contour C , with complex permittivity ϵ_2 . Wavenumbers in the two regions are $k_i = \omega \sqrt{\mu_0 \epsilon_i}$ for $i = 1, 2$. Unit normal vectors to the interface contour C are chosen as $\hat{n}_{1,2}$, directed outward from the respective regions, such that $\hat{n}_2 = -\hat{n}_1 = \hat{n}$. A coordinate system is chosen with the z -axis normal to the sea plane, while the sea surface is uniform along y and periodic along x as $z(x) = -h \cos(2\pi x/L)$ with h the sea height and L its period.

The transverse magnetic scattering problem is of greatest interest, due to the potential absence of specular reflections at the Brewster's incidence angle. For the TM polarization, all EM fields can be expressed in terms of the generating field $\vec{H} = \hat{y}H_y(x,z) = \hat{y}\psi(x,z)$. Surface field ψ and its normal derivative satisfy the coupled integral equations (where $\vec{\rho} = \hat{x}x + \hat{z}z$ is the 2-D position vector)

$$\frac{\psi(\vec{\rho})}{2} - PV \int_{C_p} \left[\psi(\vec{\rho}') \frac{\partial G_1(\vec{\rho}|\vec{\rho}')}{\partial n'} - \frac{\partial \psi(\vec{\rho}')}{\partial n'} G_1(\vec{\rho}|\vec{\rho}') \right] dl' = \psi'(\vec{\rho})$$

$$\frac{\psi(\vec{\rho})}{2} + PV \int_{C_p} \left[\psi(\vec{\rho}') \frac{\partial G_2(\vec{\rho}|\vec{\rho}')}{\partial n'} - \frac{\epsilon_2}{\epsilon_1} \frac{\partial \psi(\vec{\rho}')}{\partial n'} G_2(\vec{\rho}|\vec{\rho}') \right] dl' = 0$$

with periodic Green's-function kernels represented in Floquet-mode series expansions. The incident magnetic field is $\psi'(\vec{\rho}) = H_0 e^{-j\beta x} e^{jqz}$ with $\beta = k_1 \sin \theta_i$, $q = k_1 \cos \theta_i$, where θ_i is the incidence angle. Notation PV implies evaluation of integrals in a principal-value sense, and C_p is the first period of the sea surface. The integral equations are solved numerically by the method of moments to obtain frequency domain spectra for the surface and scattered fields. Results are compared with those obtained from an approximate Floquet-mode-matching analysis based upon the Rayleigh approximation; agreement is found to be excellent within the regime of the latter approximation.

The frequency-domain spectra are used to construct the time-domain pulse response of the sea surface using the inverse FFT. Results are found to be significantly influenced by cutoff frequencies associated with the Floquet modes. For the backscattered field, each such mode has a lower cutoff frequency, below which it becomes evanescent in the z -direction, and an upper cutoff frequency, above which it becomes forward propagating. Extensive numerical results are obtained.

**SCATTERING OF PULSED RADIATION
FROM AN IMPERFECTLY-CONDUCTING
PERIODIC SEA SURFACE**

J. Song, A. Norman, D. Nyquist, J. Ross
P. Ilavarasan, M. Seneski, K. Chen and E. Rothwell

Department of Electrical Engineering
Michigan State University
East Lansing, Michigan 48824

NATIONAL RADIO SCIENCE MEETING

5-8 January, 1994

University of Colorado
Boulder, Colorado

Session B-9, Scattering II
Paper No. 8

1. Introduction

- Scattering of pulsed electromagnetic (EM) radiation from imperfectly-conducting, periodic sea surface.
- Relevant to detection and discrimination of targets adjacent to sea-surface environment using broadband pulsed radiation.
- Attempt to mitigate effects of sea clutter upon target detection by synthesis of optimal transmit-pulse waveforms (CRTW).
- Time-domain transient response synthesized from frequency-domain transfer functions for induced surface and scattered fields.
- Approximate analysis based upon Floquet-mode expansions and Rayleigh approximation.
- Magnetic-field integral equation (MFIE) formulation based upon periodic Green's function (PGF), including numerical MoM solution.
- Transverse magnetic (TM or E-parallel) polarization studied due to potential importance of Brewster-angle phenomenon.
- Interesting cutoff phenomena associated with the spectral scattered field are identified.

2. Geometrical Configuration of Sea Surface and Basic Formulation of the 2-D Scattering Problem

- Two-medium scattering problem consists of space and sea-water regions separated by periodic sea surface (height h , period L) illuminated by plane wave incident from the space region.

$$z(x) = -h \cos(2\pi x/L)$$

- Space region is region (1), located above sea-surface contour C , with permittivity $\epsilon_1 = \epsilon_0$. Sea water is region (2), located below sea-surface contour C , with complex permittivity ϵ_2 .

$$k_i = \omega \sqrt{\mu_0 \epsilon_i} \quad \text{for } i = 1, 2$$

- Normal vectors to the interface contour C :

\hat{n}_1 directed outward from region (1)

\hat{n}_2 directed outward from region (2)

$$\hat{n}_2 = -\hat{n}_1 = \hat{n}$$

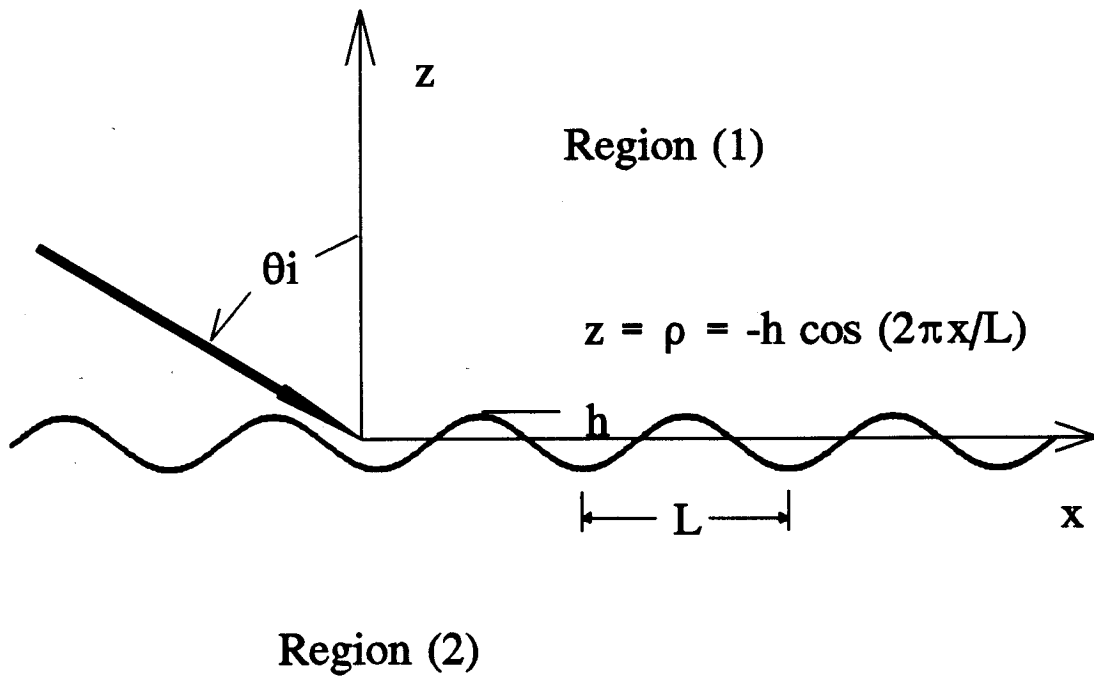


Figure 1. Configuration of periodic sea surface and incident plane wave.

- TM polarization--all EM fields can be expressed in terms of the generating field $H_y(x,z)$.

$$\vec{E} = \hat{x}E_x(x,z) + \hat{z}E_z(x,z)$$

$$\vec{H} = \hat{y}H_y(x,z)$$

$$\nabla_t^2 H_{yi}(x,z) + k_i^2 H_{yi}(x,z) = -\hat{y} \cdot \nabla_t \times \vec{J}(x,z) \quad \dots \text{for } i=1,2 \quad (1)$$

$$\vec{E}_i(x,z) = \frac{j}{\omega \epsilon_i} \hat{y} \times \nabla_t H_{yi}(x,z) \quad (2)$$

$$\nabla_t = \hat{x} \frac{\partial}{\partial x} + \hat{z} \frac{\partial}{\partial z} = \text{2-D transverse differential operator}$$

- Incident plane wave field:

$$H_y^i(x,z) = H_0 e^{-j\beta x} e^{jqz} \quad (3)$$

$$\beta = k_1 \sin \theta_i ; \quad q = k_1 \cos \theta_i$$

- Boundary conditions on tangential \vec{H} and \vec{E} , at points along sea-surface interface contour, C lead to:

$$H_{y2} = H_{y1}$$

$$\frac{\partial H_{y2}}{\partial n} = \frac{\epsilon_2}{\epsilon_1} \frac{\partial H_{y1}}{\partial n} \quad (4)$$

3. Floquet-Mode-Matching Formulation with Rayleigh Approximation

- TM-polarized incident plane-wave illumination, with total fields:

$$\begin{aligned} H_{y1}(x,z) &= H_1^i(x,z) + H_1^s(x,z) \\ H_{y2}(x,z) &= H_2^s(x,z) \end{aligned} \quad (5)$$

- Floquet-mode-series scattered field representations with $\beta_n = \beta + \frac{2n\pi}{L}$:

$$H_\alpha^s(x,z) = \sum_{n=-\infty}^{\infty} e^{-j\beta_n x} f_{\alpha n}(z) \quad \dots \text{ for } \alpha = 1,2 \quad (6)$$

- Formulation based upon Rayleigh approximation:

$$\sum_{n=-\infty}^{\infty} e^{-j\beta_n x} \left(\frac{\partial^2}{\partial z^2} + q_{\alpha n}^2 \right) f_{\alpha n}(z) = 0 \quad (7)$$

$$q_{\alpha n}^2 = k_\alpha^2 - \beta_n^2 \quad \dots \quad \text{Im}\{q_{\alpha n}\} < 0$$

$$\frac{\partial^2 f_{\alpha n}}{\partial z^2} + q_{\alpha n}^2 f_{\alpha n} = 0 \quad (8)$$

Rayleigh hypothesis: $f_{1n}(z)$ = wave travelling upward in +z direction.

$f_{2n}(z)$ = wave travelling downward in -z direction.

$$H_1^s(x,z) = \sum_{n=-\infty}^{\infty} B_n e^{-j\beta_n x} e^{-jq_{1n} z} \quad (9)$$

$$H_2^s(x,z) = \sum_{n=-\infty}^{\infty} C_n e^{-j\beta_n x} e^{jq_{2n} z} \quad (10)$$

● Implementation of boundary conditions at $z = \rho(x)$:

$$\rho(x) = -h \cos\left(\frac{2\pi x}{L}\right) \quad \hat{n} = \left(\hat{z} - \hat{x} \frac{\partial \rho}{\partial x} \right) \left[1 + \left(\frac{\partial \rho}{\partial x} \right)^2 \right]^{-1/2}$$

$$H_1^i + H_1^s = H_2^s \quad (11)$$

$$-\frac{\partial \rho}{\partial x} \frac{\partial}{\partial x} (H_1^i + H_1^s) + \frac{\partial}{\partial z} (H_1^i + H_1^s) = \frac{\epsilon_1}{\epsilon_2} \left[-\frac{\partial \rho}{\partial x} \frac{\partial H_2^s}{\partial x} + \frac{\partial H_2^s}{\partial z} \right] \quad (12)$$

- Exploit field representations (3), (9) and (10) in boundary conditions (11) and (12), and apply to each the testing operator

$$\int_0^L e^{j2m\pi x/L} \{ \dots \} dx \quad \dots \quad \forall |m| \leq N \quad (13)$$

to implement Galerkin's method. Truncating the series leads to a pair of $(2N+1) \times (2N+1)$ coupled matrix equations

$$\sum_{n=-N}^N K_{1mn} B_n + \sum_{n=-N}^N K_{2mn} C_n = H_0 A_m \quad (14)$$

$$\sum_{n=-N}^N L_{1mn} B_n - \frac{\epsilon_1}{\epsilon_2} \sum_{n=-N}^N L_{2mn} C_n = H_0 D_m \quad (15)$$

or

$$\begin{bmatrix} L_{1mn} & -L_{2mn} \epsilon_1 / \epsilon_2 \\ K_{1mn} & K_{2mn} \end{bmatrix} \begin{bmatrix} B_n \\ C_n \end{bmatrix} = \begin{bmatrix} H_0 D_m \\ H_0 A_m \end{bmatrix} \quad (16)$$

where

$$K_{1mn} = - \int_0^L e^{j2\pi(m-n)x/L} e^{-jq_{1n}\rho} dx \quad (17)$$

$$K_{2mn} = - \int_0^L e^{j2\pi(m-n)x/L} e^{jq_{2n}\rho} dx \quad (18)$$

$$A_m = \int_0^L e^{j2\pi mx/L} e^{jq\rho} dx \quad (19)$$

and

$$L_{1mn} = \beta_n I_{mn}^{(1)} - q_{1n} I_{mn}^{(2)} \quad (20)$$

$$L_{2mn} = \beta_n I_{mn}^{(3)} + q_{2n} I_{mn}^{(4)} \quad (21)$$

$$D_m = -\beta I_m^{(5)} - q I_m^{(6)} \quad (22)$$

$$I_{mn}^{(1)} = \int_0^L \frac{\partial \rho}{\partial x} e^{j2\pi(m-n)x/L} e^{-jq_{1n}\rho} dx \quad (23)$$

$$I_{mn}^{(2)} = \int_0^L e^{j2\pi(m-n)x/L} e^{-jq_{1n}\rho} dx \quad (24)$$

$$I_{mn}^{(3)} = \int_0^L \frac{\partial \rho}{\partial x} e^{j2\pi(m-n)x/L} e^{jq_{2n}\rho} dx \quad (25)$$

$$I_{mn}^{(4)} = \int_0^L e^{j2\pi(m-n)x/L} e^{jq_{2n}\rho} dx \quad (26)$$

$$I_m^{(5)} = \int_0^L \frac{\partial \rho}{\partial x} e^{j2\pi mx/L} e^{jq\rho} dx \quad (27)$$

$$I_m^{(6)} = \int_0^L e^{j2\pi mx/L} e^{jq\rho} dx \quad (28)$$

4. Magnetic-Field Integral-Equation (MFIE) Formulation

- Scattered fields in regions (1) and (2) can be expressed in terms of the surface values of H_y and $\partial H_y/\partial n$ at points along the interface contour C .

$H_{y1,2} = \psi_{1,2}$ = fields in regions (1,2) and at points approaching interface contour C from the region (1,2) side.

- Desire a pair of simultaneous integral equations for the latter surface-field quantities.
- (2-D) Green's functions for unbounded homogeneous media having wavenumbers k_i for $i = 1,2$.

Aperiodic Green's function:

$$\left(\nabla_i^2 + k_i^2\right) \tilde{G}_i(x,z|x',z') = -\delta(x-x') \delta(z-z') \quad (29)$$

$$\tilde{G}_i(x,z|x',z') = \frac{-j}{4} H_0^{(2)}\left(k_i \sqrt{(x-x')^2 + (z-z')^2}\right) \quad (30)$$

Periodic Green's function:

$$\begin{aligned} (\nabla_t^2 + k_i^2) G_i(x, z | x', z') \\ = \sum_{n=-\infty}^{\infty} e^{-j\beta n L} \delta[x - (x' + nL)] \delta(z - z') \end{aligned} \quad (31)$$

$$G_i(x, z | x', z') = -\frac{j}{2L} \sum_{n=-\infty}^{\infty} \frac{e^{-j\beta_n(x-x')} e^{-jq_{in}|z-z'|}}{q_{in}} \quad (32)$$

$$\beta_n = \beta + \frac{2n\pi}{L}, \quad q_{in}^2 = k_i^2 - \beta_n^2, \quad q_{in} = -j\sqrt{\beta_n^2 - k_i^2} \dots \text{Im}\{q_{in}\} < 0$$

- **Field in region (1).** Replace region (2) by equivalent polarization currents $\vec{J}_{eq}^{(2)} = j\omega(\epsilon_2 - \epsilon_1)\vec{E}_2$ immersed, along with primary current \vec{J} , in homogeneous medium (1). Polarization currents in region (2) are subsequently replaced by equivalent surface sources over contour C . Applying 2-D Green's theorem leads to

$$\psi_1(\vec{\rho}) = \psi_1^i(\vec{\rho}) + \int_{C_P} \left[\psi_1(\vec{\rho}') \frac{\partial G_1(\vec{\rho} | \vec{\rho}')}{\partial n'} - G_1(\vec{\rho} | \vec{\rho}') \frac{\partial \psi_1(\vec{\rho}')}{\partial n'} \right] dl' \quad (33)$$

C_p is the sea-surface contour in its first period for $0 \leq x \leq L$.

$$\psi_1^i(\vec{\rho}) = \int_{CS} [\hat{y} \cdot \nabla_t' \times \vec{J}(\vec{\rho}')] \tilde{G}_1(\vec{\rho} | \vec{\rho}') dS' \quad (34)$$

$$\psi_1^i(\vec{\rho}) = H_0 e^{-j\beta x} e^{jqz} \dots \text{ for remote source currents} \quad (35)$$

When $\vec{\rho}$ is a point on C , accommodating the source-point singularity leads to

$$\begin{aligned} \frac{\psi_1(\vec{\rho})}{2} = \psi_1^i(\vec{\rho}) + PV \int_{C_p} \left[\psi_1(\vec{\rho}') \frac{\partial G_1(\vec{\rho} | \vec{\rho}')}{\partial n'} \right. \\ \left. - G_1(\vec{\rho} | \vec{\rho}') \frac{\partial \psi_1(\vec{\rho}')}{\partial n'} \right] dl' \end{aligned} \quad (36)$$

where PV indicates that the integral must be evaluated in a principal-value sense by excluding a small neighborhood centered at field point $\vec{\rho}' = \vec{\rho}$.

- **Field in region (2).** Replace region (1) with equivalent polarization currents $\vec{J}_{eq}^{(1)} = j\omega(\epsilon_1 - \epsilon_2)\vec{E}_1$ immersed in a homogeneous medium (2). Primary and polarization currents in region (1) are then replaced by equivalent surface sources over interface contour C . Applying the 2-D Green's theorem leads, for field points $\vec{\rho} \in C$ to

$$\frac{\psi_2(\vec{\rho})}{2} = -PV \int_{C_P} \left[\psi_2(\vec{\rho}') \frac{\partial G_2(\vec{\rho} | \vec{\rho}')}{\partial n'} - G_2(\vec{\rho} | \vec{\rho}') \frac{\partial \psi_2(\vec{\rho}')}{\partial n'} \right] dl' \quad (37)$$

● Boundary conditions (4) require

$$\psi_2 = \psi_1 = \psi, \quad \frac{\partial \psi_2}{\partial n} = \frac{\epsilon_2}{\epsilon_1} \frac{\partial \psi_1}{\partial n} = \frac{\epsilon_2}{\epsilon_1} \frac{\partial \psi}{\partial n} \quad (38)$$

along contour C , where ψ and $\partial\psi/\partial n$ are regarded as unknown. Implementing these boundary conditions in Eqs. (36) and (37) leads, for all $\vec{\rho} \in C_P$, to the dual MFIE's

$$\frac{\psi(\vec{\rho})}{2} - PV \int_{C_P} \left[\psi(\vec{\rho}') \frac{\partial G_1(\vec{\rho} | \vec{\rho}')}{\partial n'} - \frac{\partial \psi(\vec{\rho}')}{\partial n'} G_1(\vec{\rho} | \vec{\rho}') \right] dl' = \psi_1^i(\vec{\rho}) \quad (39)$$

$$\frac{\psi(\vec{\rho})}{2} + PV \int_{C_P} \left[\psi(\vec{\rho}') \frac{\partial G_2(\vec{\rho} | \vec{\rho}')}{\partial n'} - \frac{\epsilon_2}{\epsilon_1} \frac{\partial \psi(\vec{\rho}')}{\partial n'} G_2(\vec{\rho} | \vec{\rho}') \right] dl' = 0 \quad (40)$$

- Scattered field in region (1):

$$\psi_1^s(\vec{\rho}) = \int_{C_P} \left[\psi(\vec{\rho}') \frac{\partial G_1(\vec{\rho} | \vec{\rho}')}{\partial n'} - \frac{\partial \psi(\vec{\rho}')}{\partial n'} G_1(\vec{\rho} | \vec{\rho}') \right] dl' \quad (41)$$

Moment-Method Numerical Solution:

- A MoM numerical solution to MFIE's (39) and (40) was implemented by expanding ψ and $\partial\psi/\partial n$ in pulse-function basis sets and subsequently testing by point matching.
- All spatial integrals are calculated in closed form.
- Floquet-mode series for the matrix elements are summed numerically. Series for matrix elements corresponding to source and field points at the same sea-surface height are very slowly convergent. The convergence of these series was accelerated by subtracting and adding the asymptotic value of the summand for large $|n|$ and summing the added series analytically.
- Subsequent to obtaining a numerical solution for the surface fields the scattered field is calculated from Eq. (41), leading to a Floquet-mode series for that field which arise from similar series in the periodic Green's function.

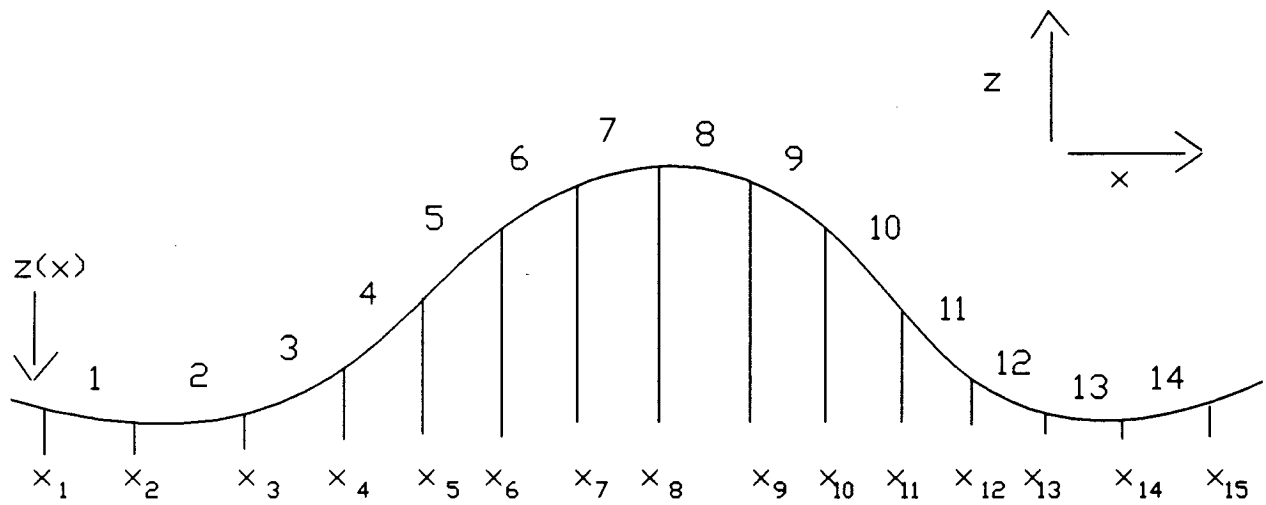


Figure 2. Method-of-moments segmentation scheme.

5. Numerical Results

- The Floquet-mode-matching formulation based upon the Rayleigh approximation was implemented.
- The MoM numerical solution for unknown surface fields was implemented.
- Both formulations lead to Floquet-mode series for the surface and scattered fields.
- The distant scattered fields exhibit interesting cutoff phenomena which dramatically influence the spectral response of the sea surface in the frequency domain, and ultimately its time-domain response to pulsed radiation.

Cutoff frequency, below which n 'th Floquet mode becomes evanescent (q_{1n} negative imaginary):

$$(f_c)_n = \frac{c |n|}{L(1 + \sin \theta_i)} \quad (42)$$

Maximal frequency, above which **backward-travelling** Floquet modes with $n = -|n|$ become forward travelling:

$$(f_{\max})_n = \frac{c |n|}{L \sin \theta_i}$$

Existence regime for non-evanescent, backward-travelling Floquet modes having $n = -|n|$:

$$(f_c)_n < f < (f_{\max})_n$$

Example: $L = 0.1016 \text{ m}$, $\theta_i = 85^\circ$

Table I Low frequency cutoff and maximal frequency of backward Floquet modes.

n	$(f_c)_n$ GHz	$(f_{\max})_n$ GHz
-1	1.479	2.964
-2	2.958	5.928
-3	4.438	8.892
-4	5.916	11.86
-5	7.395	14.82

- Time-domain band-limited impulse responses are calculated as IFT's of spectral fields. Frequency spectrum of $1.0 \text{ GHz} < f < 7.0 \text{ GHz}$ used for most numerical results.

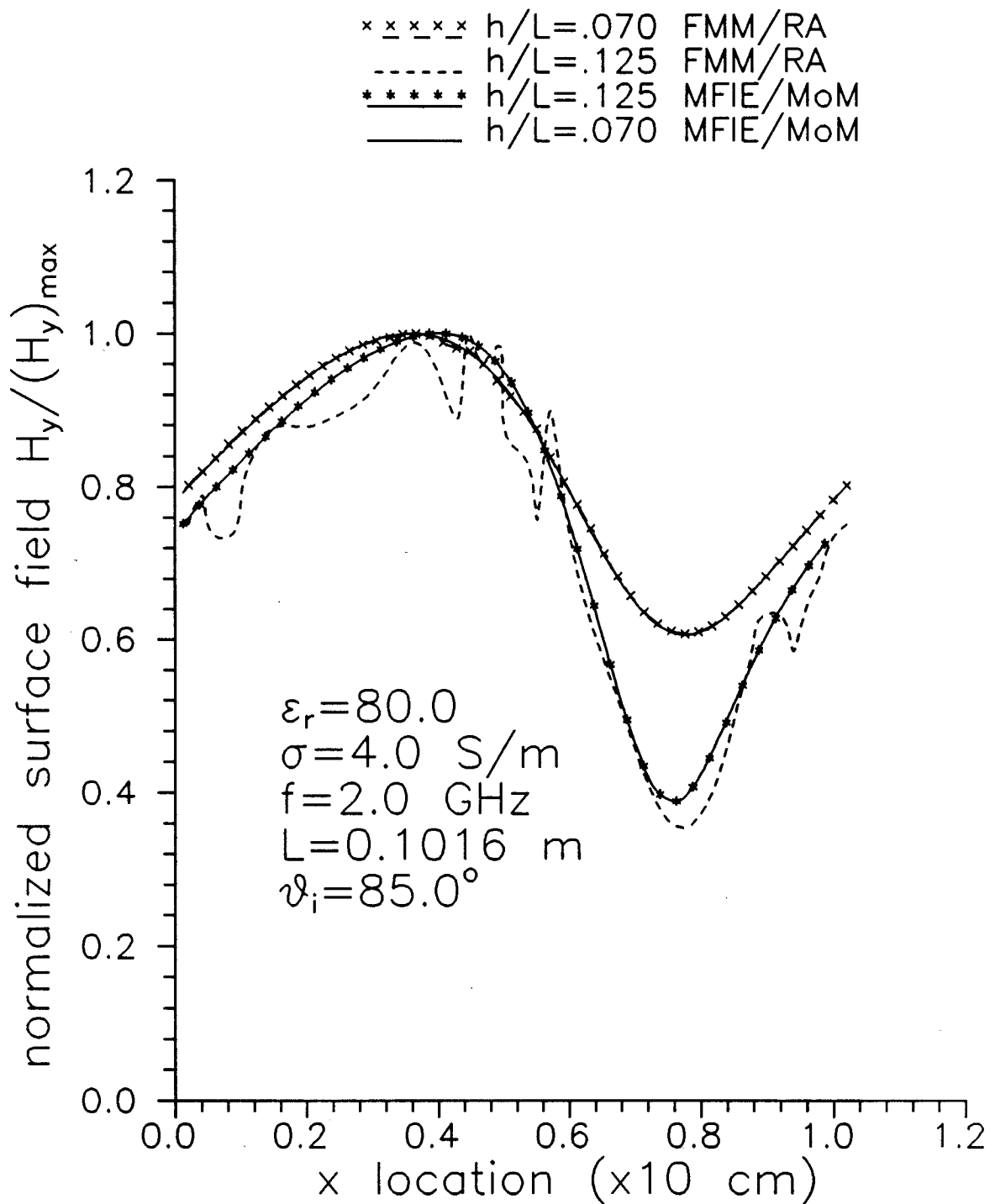


Figure 3. Comparison of surface fields calculated by Floquet mode matching with Rayleigh approximation (FMM/RA) and moment-method solution to magnetic-field integral equation (MFIE/MoM).

$\epsilon_r = 80.0$ $L = 0.1016$ m
 $\sigma = 0.0$ S/m $f = 2.0$ GHz

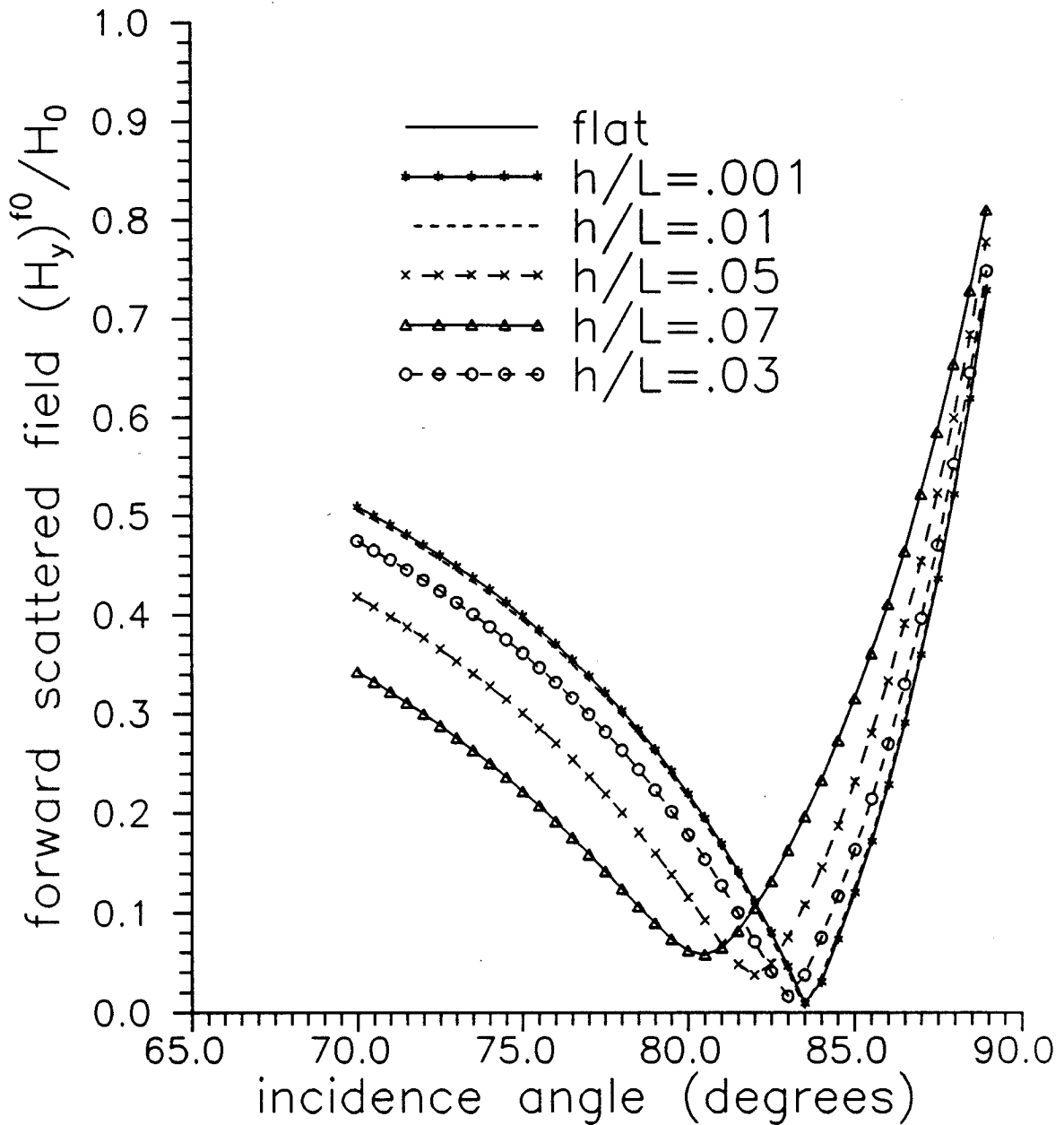


Figure 4. Identification of Brewster's angle for lossless periodic sea surface, based upon Floquet mode-matching formulation ($n=0$ mode) with Rayleigh approximation.

$\epsilon_r=80.0$ $L=0.1016$ m
 $\sigma=4.0$ S/m $f=2.0$ GHz

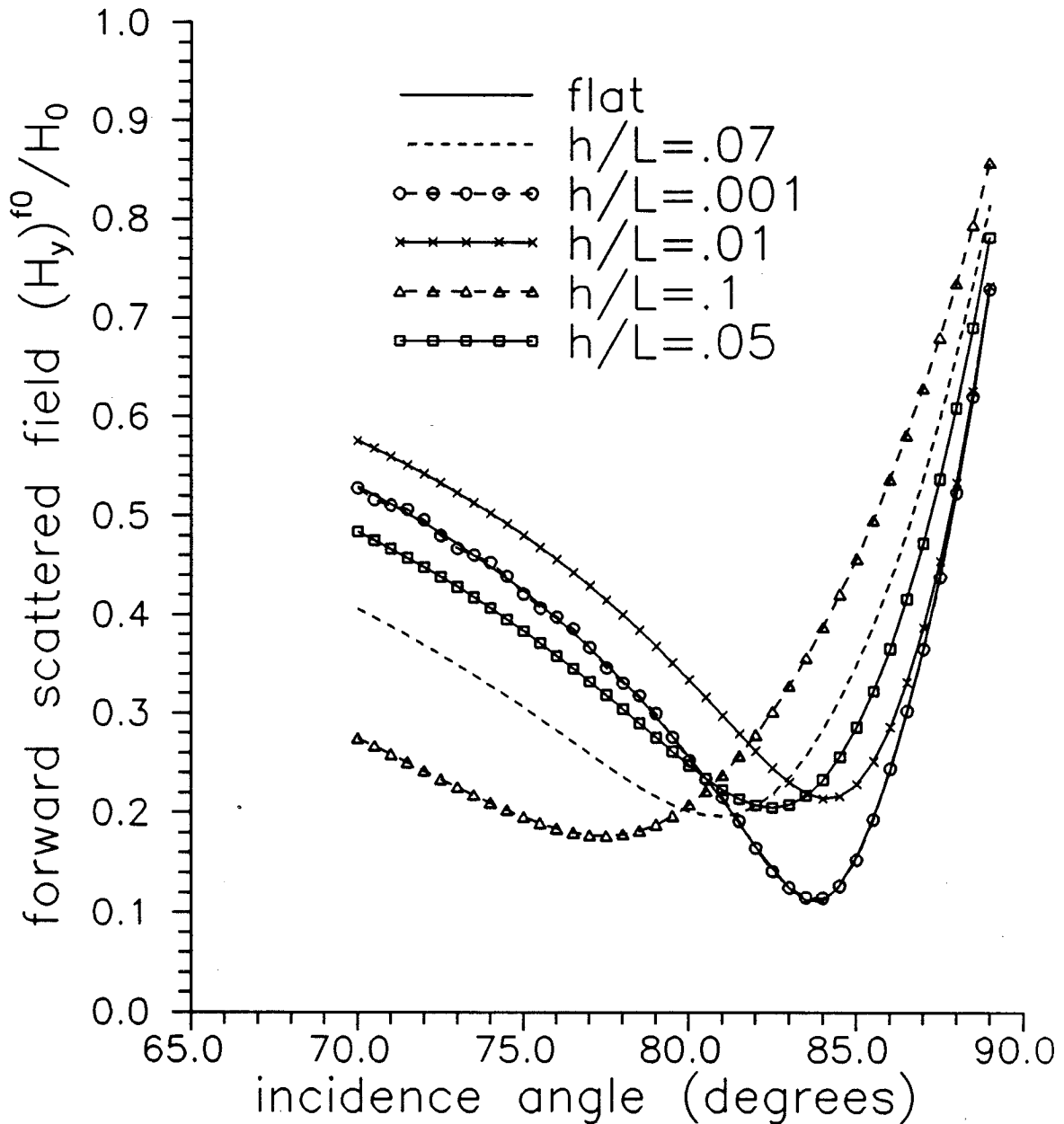


Figure 5. Identification of Brewster's angle for lossy periodic sea surface, based upon Floquet mode-matching formulation ($n=0$ mode) with Rayleigh approximation.

$\epsilon_r = 80.0$ $L = 0.1016$ m
 $\sigma = 4.0$ S/m $f = 2.0$ GHz

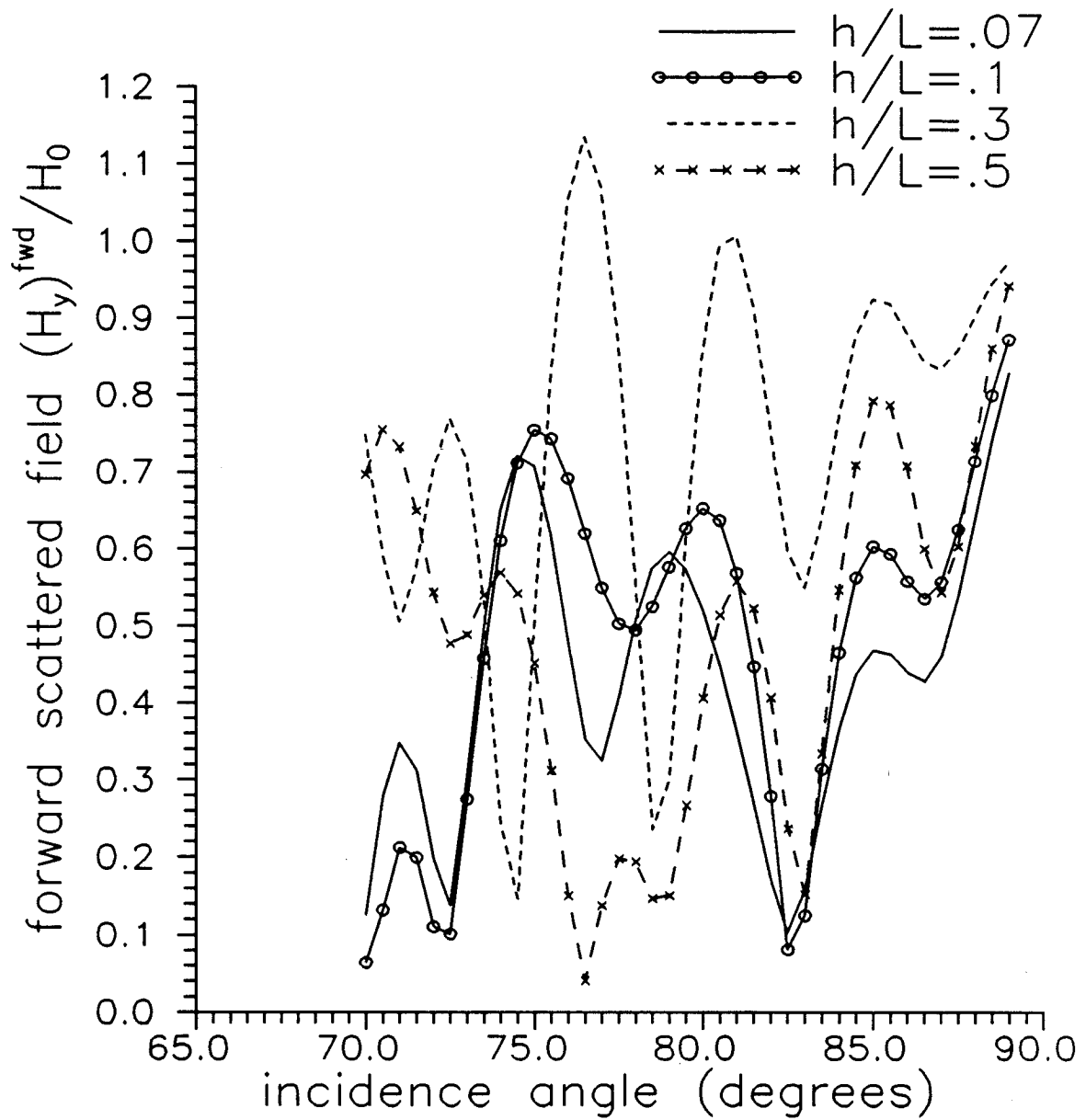


Figure 6. Identification of Brewster angle from total forward scattered field (lossy periodic sea); calculated from moment method solution to magnetic-field integral equations (MFIE/MoM).

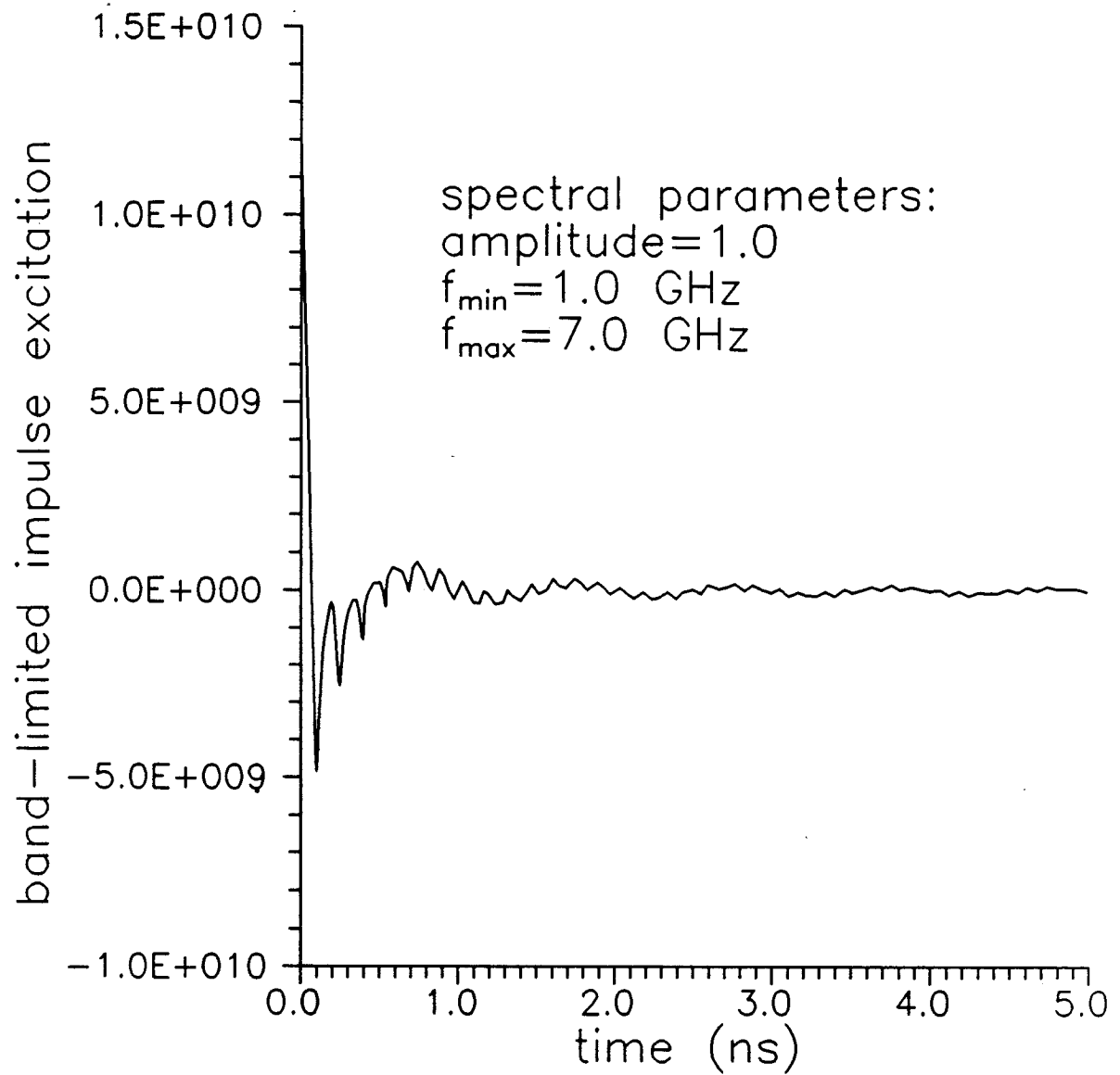


Figure 7. Band-limited, impulsive, time-domain incident plane-wave excitation.

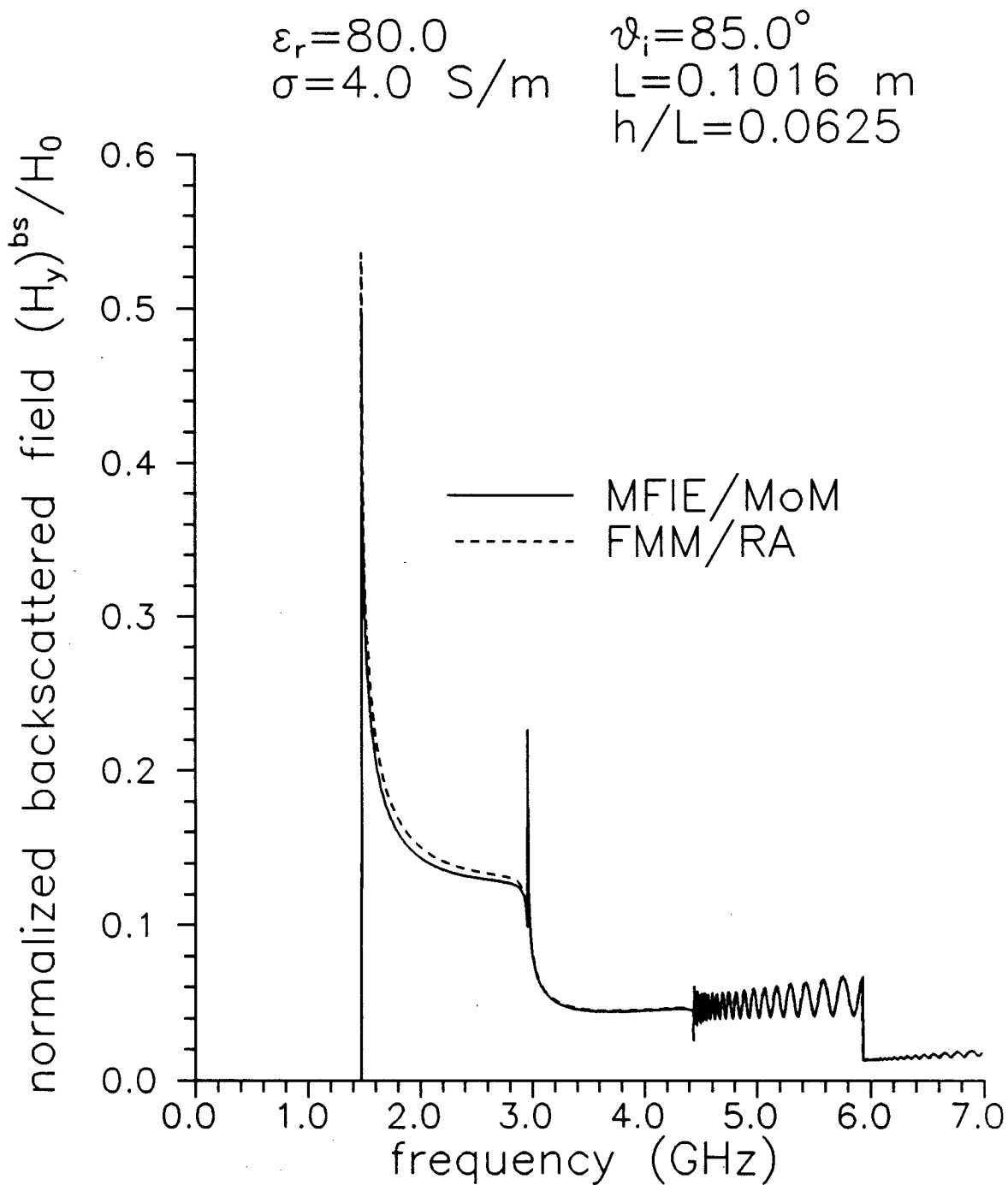


Figure 8. Frequency spectra for backscattered TM response of lossy sea surface to plane-wave excitation; Floquet mode matching with Rayleigh approximation (FMM/RA) and MoM solution to magnetic-field integral equation (MFIE/MoM).

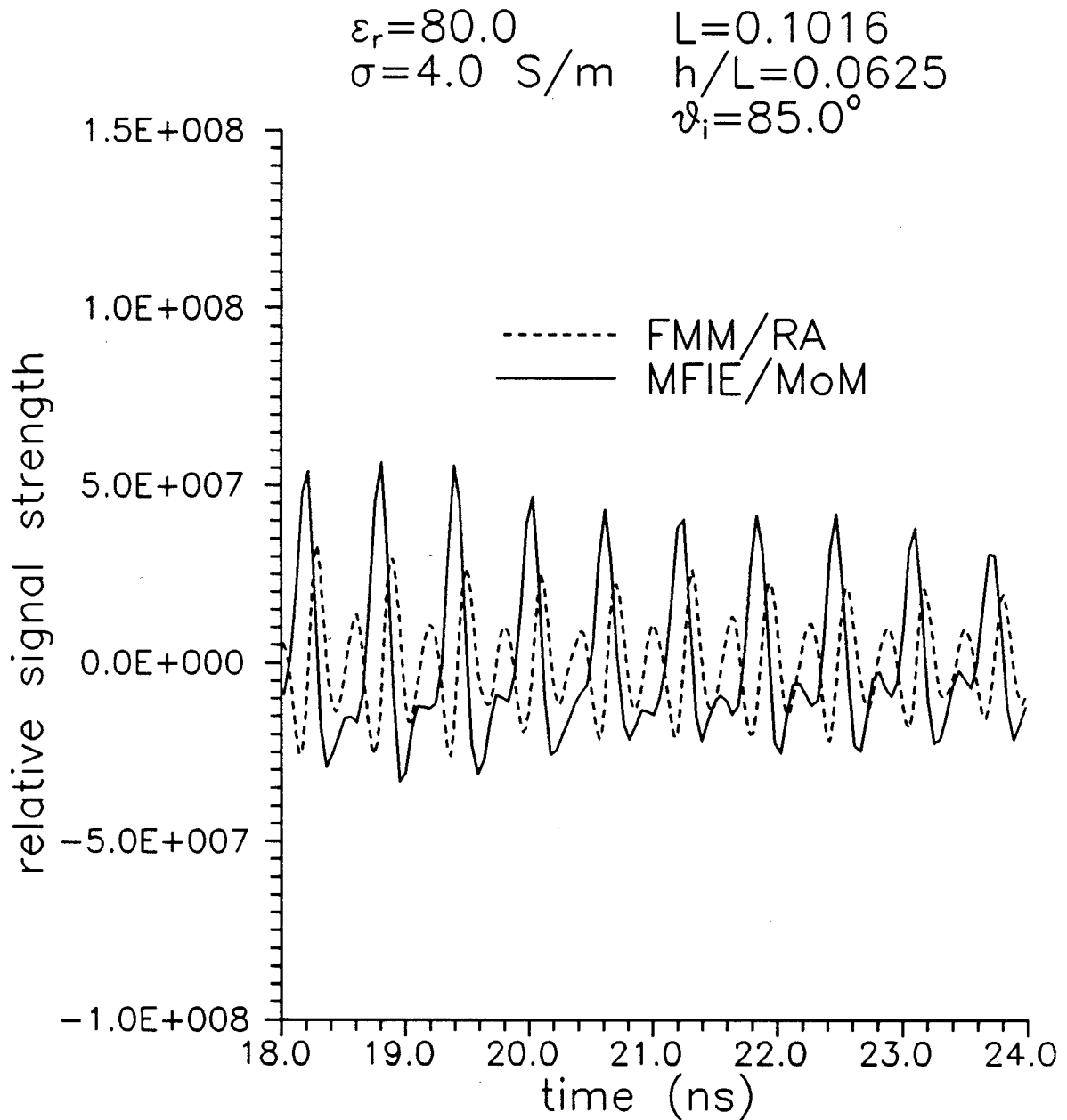


Figure 9. Time-domain backscattered TM response of lossy periodic sea surface to impulsive plane-wave excitation; Floquet mode matching with Rayleigh approximation (FMM/RA) and MoM solution to MFIE's (MFIE/MoM).

$\epsilon_r = 80.0$ $\vartheta_i = 85.0^\circ$
 $\sigma = 4.0 \text{ S/m}$ $L = 0.1016 \text{ m}$
 $h/L = 0.0625$

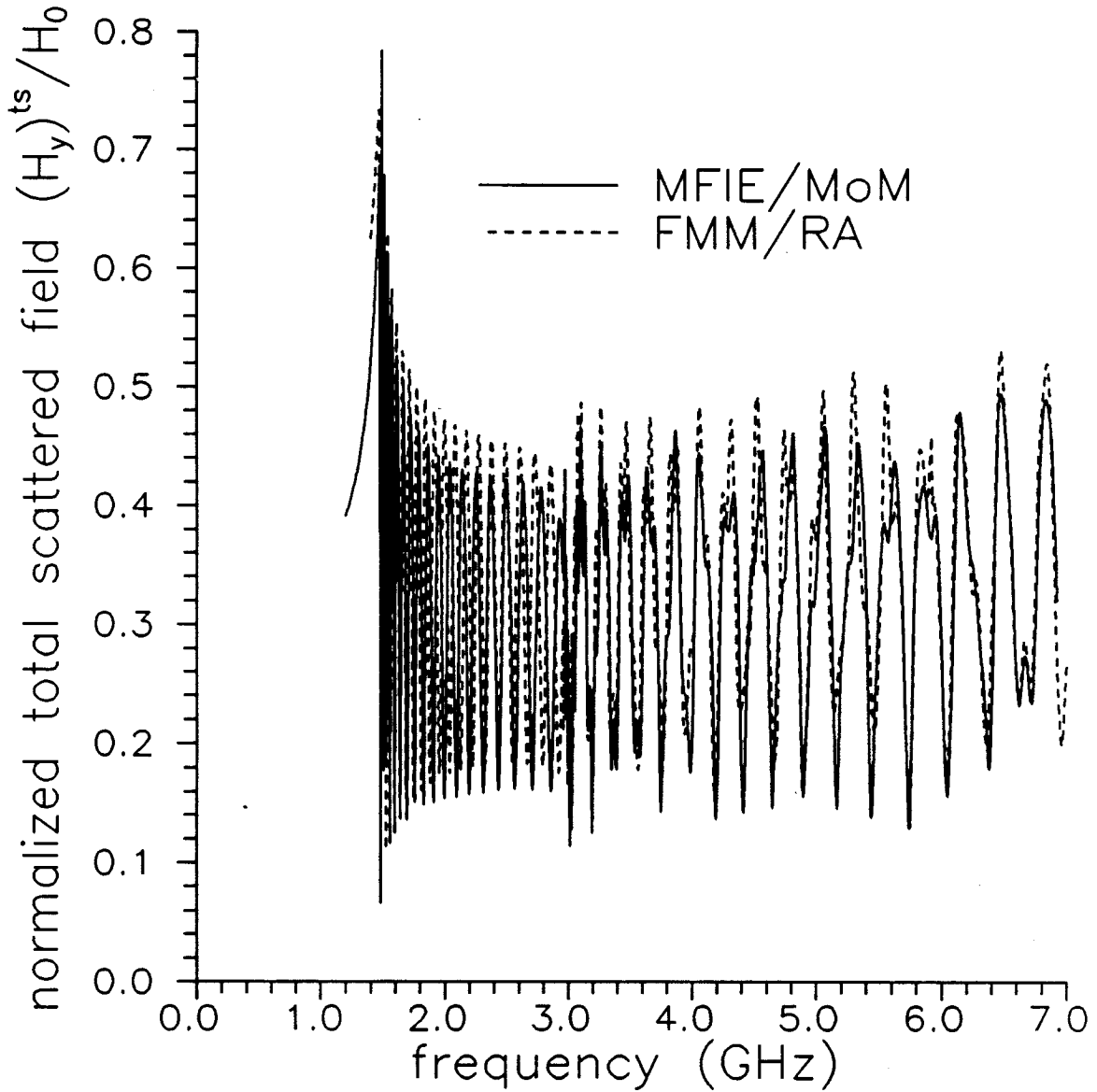


Figure 10. Comparison of frequency spectra for total scattered fields calculated by Floquet mode matching with Rayleigh approximation (FMM/RA) and moment-method solution to magnetic-field integral equation (MFIE/MoM).

$\epsilon_r=80.0$ $L=0.1016$ m
 $\sigma=4.0$ S/m $h/L=0.0625$
 $\vartheta_i=85.0^\circ$

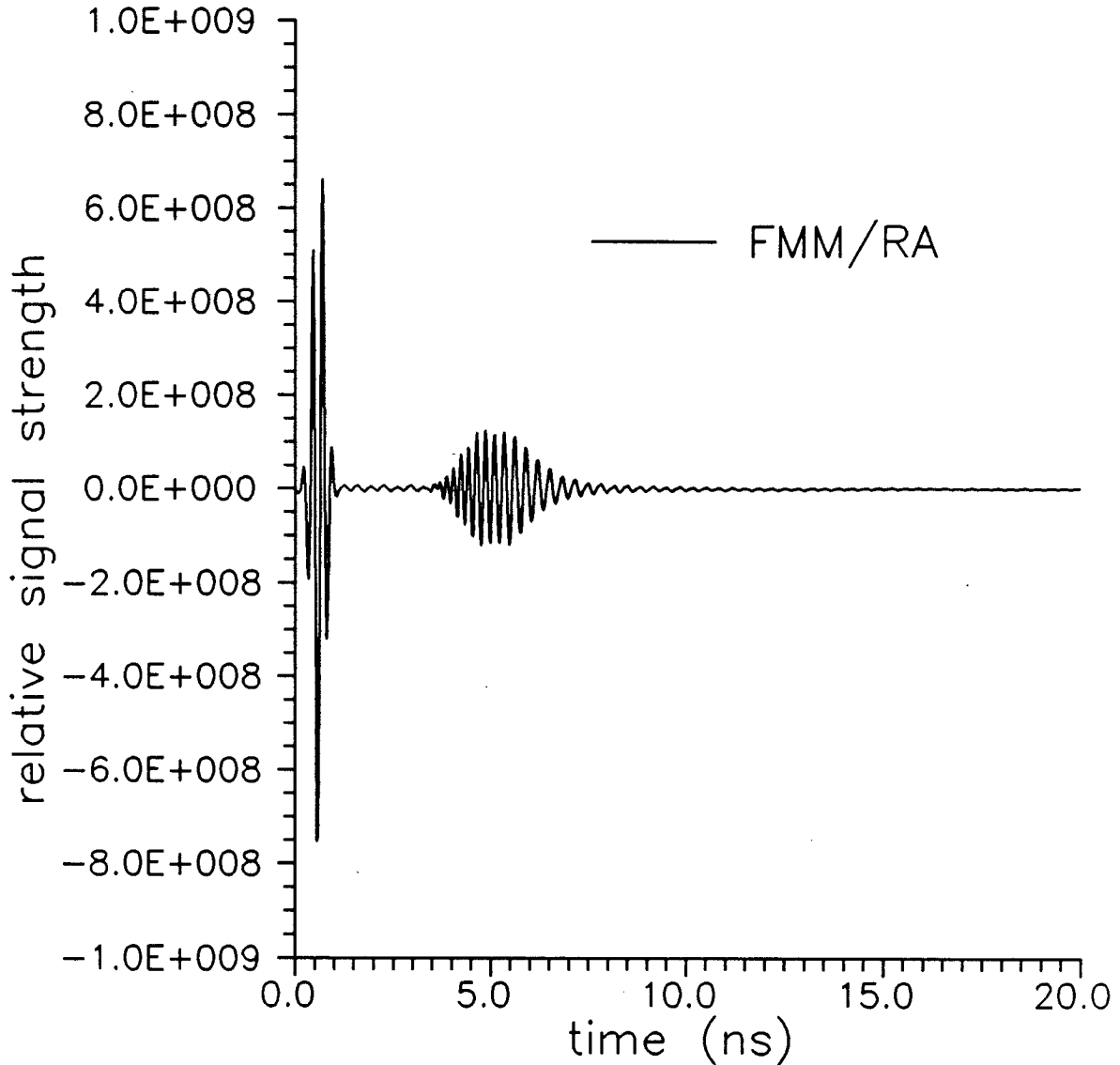


Figure 11. Time-domain total TM response of imperfectly-conducting periodic sea surface to impulsive plane-wave excitation; calculated using Floquet mode matching with Rayleigh approximation (FMM/RA).

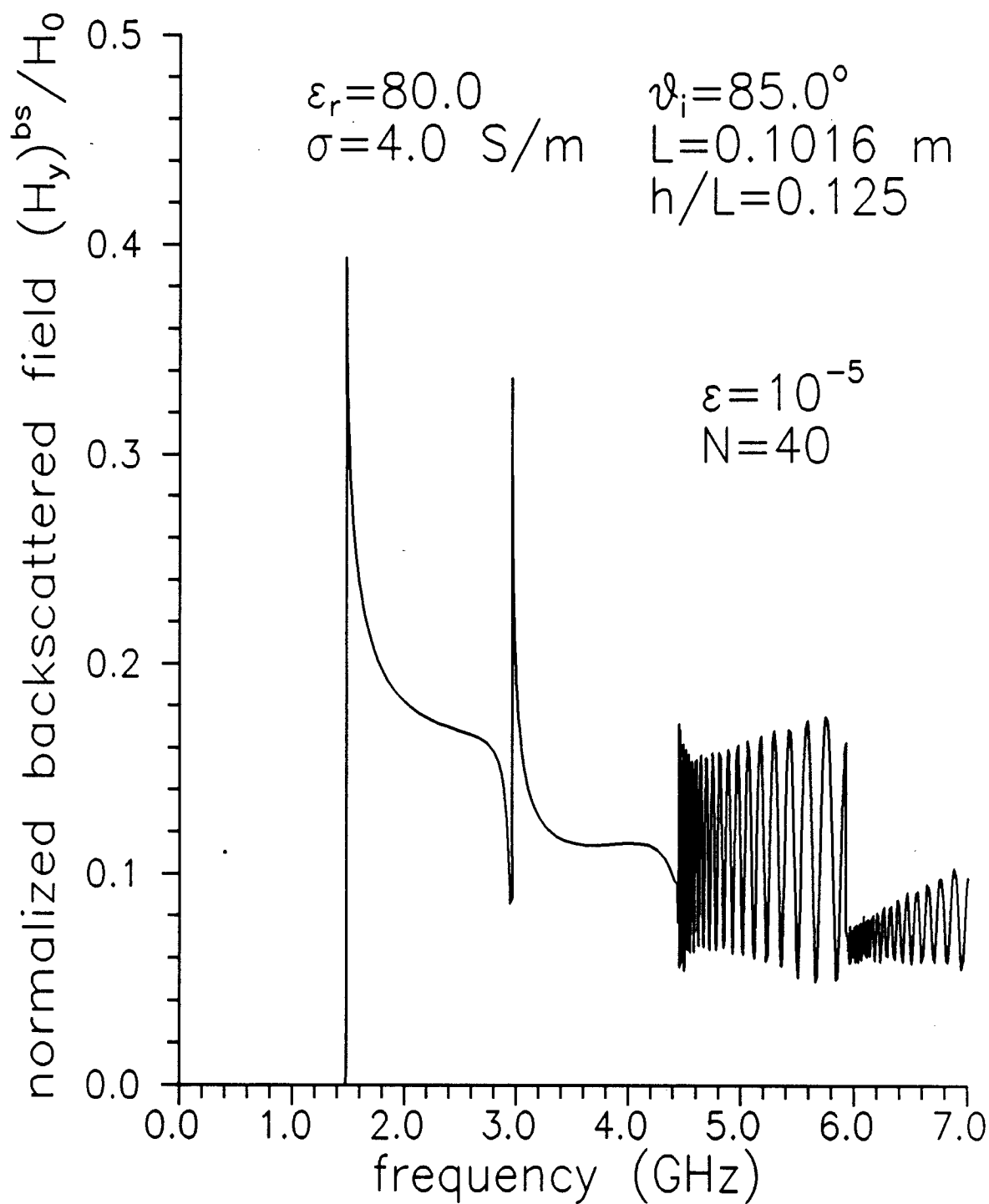


Figure 12. Frequency spectrum for backscattered TM response of imperfectly-conducting periodic sea surface to plane-wave excitation; calculated using MoM solution to coupled MFIE's (MFIE/MoM).

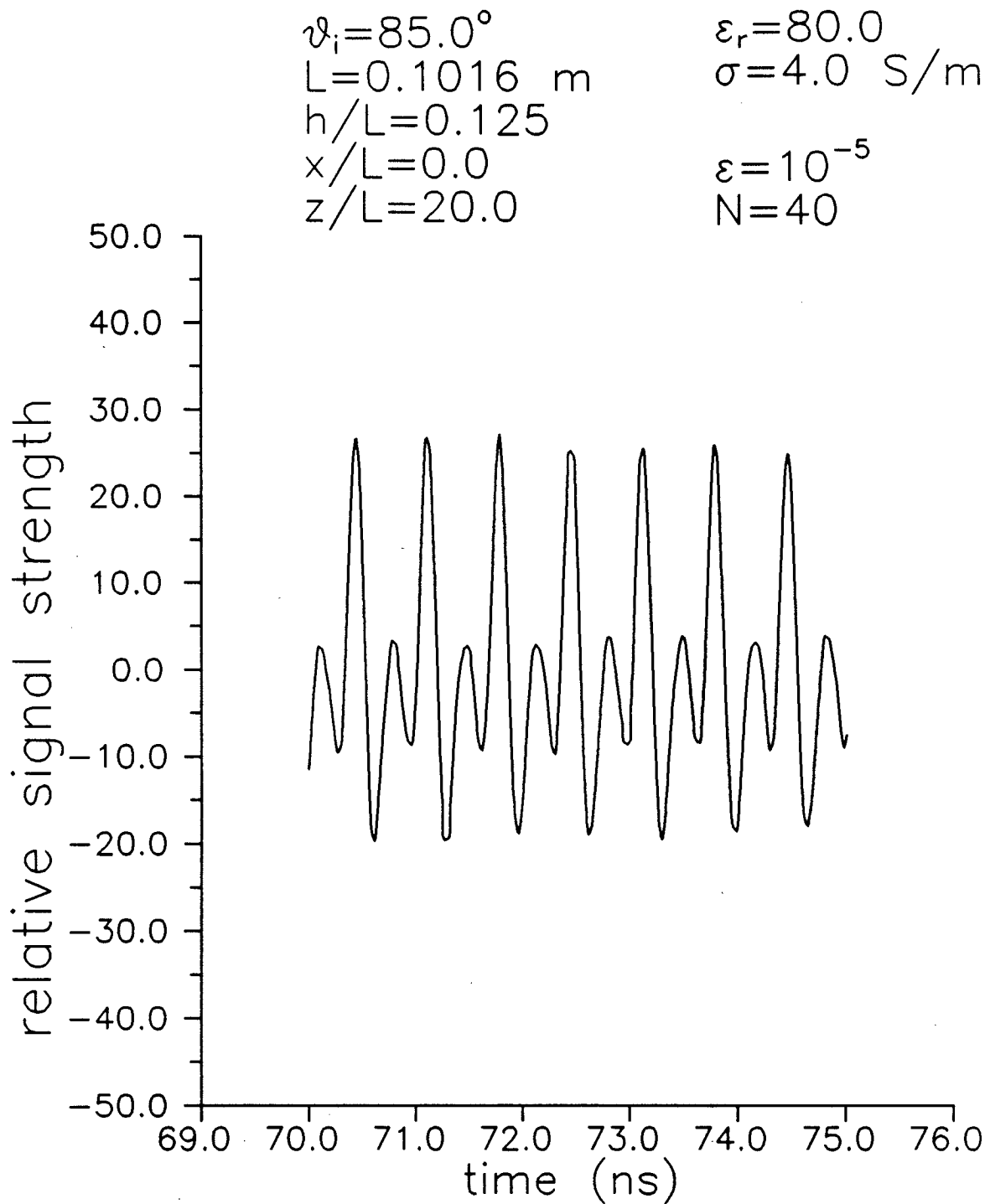


Figure 13. Time-domain backscattered TM response of imperfectly-conducting periodic sea surface to impulsive plane-wave excitation; calculated using MoM solution to coupled MFIE's (MFIE/MoM).